ABA is required for differential cell wall acidification associated with root hydrotropic bending in tomato

Ying Li[1, #], Yadi Chen[2, #], Shuqiu Jiang[1, #], Hui Dai[3], Weifeng Xu[3, *], Qian Zhang[3], Jianhua Zhang[4], Ian C. Dodd[5, *], Wei Yuan[3, *]

[1]Jiangsu Key Laboratory of Crop Genomics and Physiology, Jiangsu Key Laboratory of Crop Cultivation and Physiology, Jiangsu Co-Innovation Center for Modern Production Technology of Grain Crops, College of Agriculture, Yangzhou University, Yangzhou 225009, China

[2]College of Horticulture and Landscape, Yangzhou University, Yangzhou 225009, China

[3]Joint International Research Laboratory of Water and Nutrient in Crops, Center for Plant Water-Use and Nutrition Regulation and College of Resource and Environment, Fujian Agriculture and Forestry University, Jinshan Fuzhou 350002, China

[4]Department of Biology, Hong Kong Baptist University, Hong Kong, China

[5]The Lancaster Environment Centre, Lancaster University, Lancaster, UK

# These authors contributed equally to this work.

[*]Corresponding author: Weifeng Xu, wfxu@fafu.edu.cn; Ian C. Dodd, i.dodd@lancaster.ac.uk; Wei Yuan, yuanwei@fafu.edu.cn.

Abstract

Hydrotropism is an important adaptation of plant roots to the uneven distribution of water, with current research mainly focused on *Arabidopsis thaliana.* To examine hydrotropism in tomato (*Solanum lycopersicum*) primary roots, we used RNA sequencing to determine gene expression of root tips (apical 5 mm) on dry and wet sides of hydrostimulated roots grown on agar plates. Hydrostimulation enhances cell division and expansion on the dry side compared to the wet side of the root tip. In hydrostimulated roots, the ABA biosynthesis gene *ABA4* was induced more on the dry than the wet side of root tips. The ABA biosynthesis inhibitor fluridone and the ABA deficient mutant *notabilis* (*not*) significantly decreased hydrotropic curvature. Wild-type, but not the ABA biosynthesis mutant *not,* root tips showed asymmetric H^+ efflux, with greater efflux on the dry than wet side of root tips. Thus ABA mediates asymmetric H^+ efflux, allowing the root to bend towards the wet side to take up more water.

KEYWORDS: ABA, proton efflux, hydrotropism, root, tomato (*Solanum lycopersicum*)

Summary statement: ABA regulates asymmetric H^+ efflux, which is required for the root hydrotropic bending.

1 INTRODUCTION

Water shortage is the major threat to agricultural production on a worldwide scale. Even in areas with sufficient water, the uneven distribution of water in the soil requires plants to continuously adapt their root system to obtain more water (Li et al., 2020 a). Root hydrotropism occurs when plant roots sense the water potential gradient in their microenvironment and direct growth towards moist soil (Takahashi et al., 2002; Li et al., 2020 b). Despite the significance of hydrotropism, our understanding of its physiological and molecular processes is very limited (Iwata et al., 2013; Eapen et al., 2017).

Abscisic acid (ABA) is a critical stress phytohormone, and the ABA signal transduction pathway (PYR/PYL/RCAR-PP2Cs-SnRK2s) plays a pivotal role in coordinating root responses to decreased water availability (Sharp et al., 1994; Antoni et al., 2013; Rowe et al., 2016; Dietrich et al., 2017). Under stress conditions, ABA is rapidly synthesised and binds to Pyrabactin resistance1/PYR1-like/regulatory components of ABA receptor (PYR/PYL/RCAR) proteins, which subsequently repress group A PROTEIN PHOSPHATASES 2Cs (PP2Cs) (Ma et al., 2009; Nishimura et al., 2009). Concurrently, subclass III sucrose non-fermenting-1 related protein kinase 2 (SnRK2s) are released from PP2C-SnRK2 complexes to phosphorylate and activate a subgroup of the basic leucine zippers (bZIPs) transcription factors including ABA insensitive 5 (ABI5) and ABFs/ AREBs that recognize the ABRE promoter element (consensus PyACGTGG/TC) in ABA-responsive genes (Uno et al., 2000; Furihata et al., 2006; Fujii et al., 2007; Ma et al., 2009; Park et al., 2009). In addition, SnRK2s kinases have many more phosphorylation targets besides transcription factors, such as ion channels (SLOW ANION CHANNEL-ASSOCIATED 1, SLAC1 and potassium channel protein, KAT1) (Umezawa et al., 2013; Wang et al., 2013). The *Arabidopsis aba1-1* mutants were less sensitive to hydrostimulation, while applying ABA to *aba1-1* restored the normal sensitivity to the hydrotropic stimulation (Takahashi et al., 2002). A sextuple ABA receptor *PYR/PYL* mutant (*112458*) showed reduced hydrotropism, whereas *Qabi2-2*

plants, a *PP2Cs* quadruple mutant, exhibited enhanced hydrotropism in *Arabidopsis* (Antoni et al., 2013). Furthermore, the SnRK2.2 kinase and *MIZU-KUSSEI 1* (*MIZ1*, a gene essential for root hydrotropism) regulate hydrotropic response in cortical cells of the elongation zone in *Arabidopsis* (Moriwaki et al., 2012; Dietrich et al., 2017). Whether these ABA-related and hydrotopism regulatory genes are asymmetrically expressed across the root in response to moisture gradients is not clear.

Plasma membrane (PM) H^+-ATPase (PM H^+-ATPase), a subfamily of P-type H^+-ATPases, generates a membrane potential and H^+ gradient across the PM, energising various ion channels and multiple H^+-coupled transporters for diverse physiological processes (Moloney et al., 1981; Hager, 2003; Falhof et al., 2016; Li et al., 2022). Various plant hormone signalling pathways are involved in regulating the activity of these plasma membrane H^+-ATPases. The brassinosteroid (BR) insensitive 1 (BRI1, a BR receptor) targets *Arabidopsis* plasma membrane (PM) H^+-dependent adenosine triphosphatase (ATPase) 2 (AHA2) to mediate hydrotropic response in *Arabidopsis*, and the *bri1-5* mutant showed reduced root hydrotropism and lower apoplastic H^+ extrusion (Miao et al., 2018). More recently, we found that ABA-insensitive 1 (ABI1), a key component of PP2C in the ABA signalling pathway, interacts directly with the C-terminal R domain of AHA2 and dephosphorylates its penultimate threonine residue (Thr^{947}), which decreases PM H^+ extrusion and negatively regulates root hydrotropic response in *Arabidopsis* (Miao et al., 2020). However, whether spatial variation in endogenous ABA biosynthesis in roots responding to moisture gradients determines expression and activity of PM H^+-ATPases, thereby mediating cellular responses during hydrotropism, has not been determined.

To understand the significance of spatial distribution of gene expression in regulating root hydrotropic bending in tomato, roots responding to a moisture gradient (imposed within agar plates) were subjected to transcriptomic analysis comprising whole root tips and those that were longitudinally split into dry (proximal to agar of lower water potential) and wet (proximal to agar of higher water potential) sides. Differential enrichment of genes involved in ABA biosynthesis and response, and

regulating H^+ efflux, was correlated with asymmetric cell elongation on opposite sides of the hydrostimulated root tips. By using an ABA biosynthesis inhibitor and the tomato ABA biosynthesis mutant *notabilis*, we tested the hypothesis that ABA mediation of PM H^+-ATPase activity determined root hydrotropism.

2 MATERIALS AND METHODS

2.1 Plant materials and growth conditions

Four tomato (*Solanum lycopersicum*) cultivars including Micro-Tom (MT), Lukullus (LU, LA0534), MM (Moneymaker), and Ailsa Craig (AC, LA2838) were used for the analysis of hydrotropism. The background of ABA-deficient mutant *notabilis* (*not*, LA0617) is LU. Tomato seeds were surface sterilized with 30% sodium hypochlorite (NaClO) and distilled water at the volume ratio of 1:2 for 3 minutes, and then rinsed with sterile distilled water 5 times. Sterile distilled water was added to the sterilized tomato seeds, and soaked at 30℃ in the dark for 2 days to ensure the seeds fully absorbed water. Subsequently, the seeds were sown on 1% agar containing 1/2 Murashige and Skoog (1/2 MS) media at 22℃ under 16 h light/ 8 h dark photoperiod. Five-day-old uniform seedlings were used for subsequent experiments.

2.2 Root hydrotropism assays

The agar-sorbitol system shown in Figure S1 was established as previously described (Takahashi et al., 2002). First, about 50 ml of 1/2 MS medium was poured into a 13 × 13 cm square dish. After it solidified, the lower left of the medium was excised with a blade (with an inclination of about 57 degrees, 2 cm from the upper and lower boundaries), and about 25 ml of 1/2 MS with sorbitol medium was poured in, with the two different media on the same level as far as possible. A water potential gradient was formed from lower left (low water potential) to upper right (high water potential) (Figures S1 and S3). The osmotic pressures of the hydrotropic experimental system was measured at various distances (a-f) from the plain agar-sorbitol (1000 mM) agar junction (Figure S3), using an Osmo310PRO cryoscopy osmometer (YASN, UK). We first marked the back of the petri dish with dashed lines (as shown in Figure S3A), and then opened the lid of the petri dish and used a scalpel to cut the agar in the petri dish along these dashed lines, and finally used the tweezers to collect samples from

the agar plates for the measurements with the osmometer. Control plates (no hydrostimulation) were initially prepared as described above, but after the 1/2 MS medium solidified, half of it was removed and replaced with the same 1/2 MS medium. Uniform tomato seedlings (the root length is about 3 cm) were positioned vertically 3 mm above the boundary between the two media. Seedlings were spaced approximately 0.6 cm apart with 10 seedlings per dish, which were sealed with film, and placed in a growth chamber. The hydrotropic bending and elongation of roots were photographed using a digital camera (Nikon D7100) and were measured using ImageJ software. Root hydrotropic bending was shown as an angle deviating from the initial straight line of the seedling root (Takahashi et al., 2002).

2.3 Treatment with exogenous ABA and ABA inhibitor Fluridone

Exogenous ABA (final concentration of 1 μM) and ABA inhibitor Fluridone (FLU) (final concentration of 10 μM) were added into 50 ml 1/2 MS medium, and poured into the square dishes. After the medium solidified, half of it was excised as described above, and about 25 ml 1/2 MS + 1000 mm sorbitol medium at the same ABA or FLU concentrations poured in. The ABA and FLU were first dissolved in ethanol, and then added to 1/2 MS medium. The final ethanol concentration in the 1/2 MS medium was 0.44% (v/v). Control plants were grown in the 1/2 MS medium with the same amount of ethanol [0.44% (v/v)].

2.4 pH determination

The pH-sensitive indicator bromocresol purple [pH range is 5.2 (yellow) to 6.8 (purple)] was used as described (Bissoli et al., 2012). Briefly, tomato plants grown on control and hydrostimulation dishes for 3 h were transferred to ½ MS vertical plates with 0.003% bromocresol purple and incubated in the light for 6-8 h. For this measurement, density of the stained areas (apical 5 mm of tomato root tips) was measured using Image J software and FastStone Capture v9.4 CHS software. Firstly, images were opened with ImageJ software, with “Image”, “color”, “Split Channels” clicked in turn, with “Green Channel” selected and saved as BMP format. Secondly, the just-saved image was opened with FastStone Capture v9.4 CHS software, with the square tool to frame the area to be processed, then the area was cropped and saved as

the image with 24-bit color. Finally, this image was re-opened with ImageJ software, with “Image”, “Type, “32-bit”, “Adjust”, “Threshold” clicked in turn, to obtain a numerical value for the relative degree of staining after adjusting the brightness of the area. The density of controls were taken to be 100%, and relative density was calculated based on control levels.

2.5 Confocal microscopy

The root tips of tomato seedlings under control conditions or hydrostimulation for 3 h were stained with propidium iodide (PI, 40 μg/mL) dye solution. After 3 h of hydrostimulation, the slightly curved root tips were placed in PI dye solution on the slide with tweezers, keeping the left and right sides of the root consistent with the growth direction on the hydrostimulation medium, and cover slips applied. The fluorescence of PI in tomato root tips was observed with a LSM 880 NLO two-photon laser confocal microscope as previously described (Xu et al., 2013). PI was excited at 553 nm and detected at 615 nm.

The root tips of tomato seedlings under normal conditions or hydrostimulation for 3 h were stained with 8-hydroxypyrene-1,3,6-trisulfonic acid trisodium salt (HPTS) (Han and Burgess, 2010; Barbez et al., 2017). The samples were soaked in 50 mm HPTS dye solution about 30 minutes, and then the samples were washed with distilled water for 3 times. The method is the same as PI. For HPTS, excitation was at 405 nm (protonation) and 458 nm (deprotonation) and emission at 514 nm. The fluorescence intensity of two channels in the elongation zone on both sides of tomato root tip was calculated using the ZEN BLUE software. In the “Measure” view, the square tool was selected in the “Graphics” tab, and the measurement area in the image defined by dragging and holding the left mouse button. After defining the area, the software automatically measured the average fluorescence intensity of each channel within this area, storing the fluorescence intensity of each channel in Excel. This ratiometric technique divides the signal intensity of the 458 nm channel of each pixel by the signal intensity of the 405 nm channel. The apoplastic pH correlates with the ratiometric values, with higher 458/405 ratios indicating higher pH and less apoplastic H^+ (Barbez et al., 2017). The intensity value is related to the proton secretion of cell

wall. Approximately 15 seedlings were imaged per group, and at least two independent experiments were performed. All images were taken under identical conditions. The density of controls were taken to be 100%, and relative density was calculated based on control levels.

2.6 Meristem cortex cell number counting

Cell numbers on both sides of the tomato root tips were counted in the meristematic zone starting from the quiescent center and ending at the onset of rapid cell elongation, by using LSM 880 NLO ZEN BLUE software after propidium iodide (PI) staining (Ivanchenko et al., 2013). The basic steps are as follows: we first selected the "Customize" option in the "Custom Graphics" tab, and then selected the "Events" tool. Next, we clicked the position to be counted continuously with the left mouse button, with the software marking "X" on the click position. Finally, the right mouse button was used for counting, with the number saved in Excel.

2.7 Elongation zone cortex cell length analyses

Cell lengths on both sides of the tomato root tips were analysed in the elongation zone, starting at the onset of rapid cell elongation and ending at the first root hair bulge in the epidermis by using ImageJ software after propidium iodide (PI) staining (Ivanchenko et al., 2013).

2.8 RNA sequencing and data analysis

The apical 5 mm of tomato root tips were obtained after 3 h of control or hydrostimulation; and the dry and wet sides of apical 5 mm of tomato root tips after 3 h of hydrostimulation were obtained by longitudinally separating the whole root into two halves with a sharp razor blade. Three biological replicate samples (with each sample comprising at least 50 roots) were taken from control conditions (Control 1, Control 2, Control 3) hydrostimulated conditions (Hydrostimulated 1, Hydrostimulated 2, Hydrostimulated 3) the dry sides of root tips grown in hydrostimulated conditions (Dry 1, Dry 2, Dry 3) and the wet sides of root tips grown in hydrostimulated conditions (Wet 1, Wet 2, Wet 3) (Figure 2). Each sample was collected into a 1.5 ml centrifuge tube without RNase, and quickly put into liquid

239 nitrogen, and then transferred to -80℃ for storage.

240 Total RNA extraction, library construction and sequencing of samples were performed
241 by Novogene Co., LTD (Beijing Nuohe Zhiyuan Technology Co., LTD). RNA
242 integrity was assessed using the RNA Nano 6000 Assay Kit of the Bioanalyzer 2100
243 system (Agilent Technologies, CA, USA). Sequencing libraries were generated using
244 NEBNext UltraTM RNA Library Prep Kit for Illumina (NEB, USA) following
245 manufacturer's recommendations and index codes were added to attribute sequences
246 to each sample. Raw data (raw reads) of fastq format were firstly processed through
247 in-house perl scripts. In this step, clean data (clean reads) were obtained by removing
248 reads containing adapter, reads containing poly(N) and low quality reads from raw
249 data. The RPKM method (reads per kilobase of transcript per million mapped reads)
250 was used to determine transcript abundance. Differential expression analysis of two
251 conditions/groups (three biological replicates per condition) was performed using the
252 DESeq2 R package (1.16.1). For each pairwise comparison, genes with $\log_2$(fold
253 change) >0.2 or <-0.2 and P-value <0.05 were considered differentially expressed
254 genes (DEGs).

255 **2.9 qRT-PCR analysis**

256 Total RNA was extracted from the apical 5 mm of tomato roots using a plant RNA Kit
257 (OMEGA, USA) according to the manufacturer's instructions. First-strand cDNA was
258 synthesized using a *TransScript* One-Step gDNA Removal and cDNA Synthesis
259 SuperMix Kit (TransGen Biotech, China) according to the manufacturer's instructions.
260 Analyses with qRT-PCR were performed using a *TransScript* Tip Green qPCR
261 SuperMix Kit (TransGen Biotech, China) and a CFX96 Real-time PCR Detection
262 system (Bio-Rad, USA) according to the manufacturers' instructions. The specific
263 primers for each gene are listed in Table S1. Results were normalized using *α-Tubulin*
264 or *Actin* gene as the endogenous control.

265 **2.10 Statistical analysis**

266 For all experiments, statistical tests were carried out using SPSS software (IBM
267 Corporation, USA). A two-tailed Student's *t*-test was used to compare between two
268 groups. For comparisons between more than two groups, Tukey's test was used. Data

were represented as the mean ± standard error (SE) from at least three independent experiments, and differences were considered significant at P-values < 0.05.

3 RESULTS

3.1 Hydrotropic bending involves differential cell elongation on dry and wet sides of tomato roots

Sorbitol induced-water potential gradients (agar-sorbitol system) are commonly employed to observe root hydrotropism in the model plant *Arabidopsis thaliana* (Takahashi et al., 2002). To find the most suitable experimental system to study tomato root hydrotropism, different water potential gradients with different concentrations of sorbitol (400 mM, 800 mM, 1000 mM, 1200 mM and 1500 mM) were used to observe root hydrotropic bending and root growth of Lukullus (LU) tomato (Figures S1 and S2). Hydrotropism of LU roots was greater in higher concentrations of sorbitol (800 mM, 1000 mM, 1200 mM and 1500 mM) than that in the 400 mM sorbitol treatment commonly used in *Arabidopsis thaliana,* with hydrotropic curvature increasing linearly to a maximum of about 45 degrees as the sorbitol concentration increased (Figure S2A). Primary root growth of LU was severely inhibited (by more than half) by the water potential gradient formed by the 1200 mM and 1500 mM sorbitol treatments (Figure S2B), but only by 43% by the 1000 mM sorbitol treatments compared with the control (Figure S2B). Since the water potential gradient formed by 1000 mM sorbitol was the most suitable system to study the hydrotropism of tomato roots, next we examined the osmotic pressures at various distances (a-f) from the plain agar-sorbitol (1000 mM) agar junction in the agar-sorbitol system (Figure S3A). Results suggest that a relatively large osmotic pressure gradient (e.g. the osmotic pressures from a to f were 367.33 ± 17.80, 492.22 ± 12.14, 640.78 ± 17.99, 810.33 ± 18.18, 999.11 ± 25.22 and 1149.56 ± 23.34 mOsm/kg) around the border between the plain and sorbitol agar plates was developed in this concentration of sorbitol after 10 hours of hydrostimulation (Figure S3B). Tomato roots initiated curvature 3 hours after the start of hydrostimulation, reaching a maximum (around 45 degrees) after 10 hours (Figure S4). In addition, we

compared the hydrotropic responses of different tomato ecotypes (Micro-Tom, LU, MM, AC). While root elongation (about 0.44 cm) was similar between these genotypes under 1000 mM sorbitol treatments, hydrotropism of the tall cultivars (LU, MM and AC) was significantly greater than the dwarf Micro-Tom cultivar (Figure S5). Thus LU was used for subsequent experiments due to seed availability and the availability of an ABA-deficient mutant.

To explore the mechanism of tomato root hydrotropic bending (Figure 1A), cortical cell growth of the meristem zone and elongation zone was observed by PI staining (Figure 1B). Under control conditions, cortex cell length did not differ between the left and right sides of the elongation zone, indicating symmetrical growth (Figures 1B and C). However, hydrostimulation resulted in asymmetric growth between the dry and wet sides of the elongation zone, with cortex cell length on the dry side 22.4% longer than on the wet side and in control plants (Figures 1B and C). The cortex cell numbers between the left and right sides of the root apical meristem zone did not differ under control conditions, but the cortex cell numbers on the dry side were significantly higher than that on the wet side under hydrostimulation (Figures 1B and D). Taken together, these results suggest that the asymmetrical growth of tomato root tips between dry and wet sides drives hydrotropic bending.

3.2 Hydrostimulation induces asymmetric expression of ABA-related genes in tomato roots

Transcriptomic analyses (RNA-sequencing) were used to identify genes involved in the early hydrotropic response (Figure 2, Figure S6) by sampling whole root tips (apical 5 mm) grown under control conditions and hydrostimulation conditions, and by longitudinally sectioning roots grown under hydrostimulation to collect samples from dry and wet sides (Figure 2A, Figure S6). Since the primary root growth of Lukullus was about 0.5 mm under hydrostimulation conditions (1000 mM sorbitol) (Figure S2B), the apical 0.5 mm was chosen as the portion for sampling. RNA sequencing analysis was conducted using three biological replicates of each treatment. In total, 12 libraries were constructed and analyzed (Figure 2A, Figure S6).

Correlation heatmap analysis showed a high Pearson correlation among the three biological replicates (Figure S6A). Furthermore, hydrostimulation induced differential gene expression (DEGs) between the dry and wet sides of tomato roots (Figure S6B).

There were 2,113 DEGs between control and hydrostimulated roots, and 198 DEGs between dry side and wet sides under the hydrostimulated treatment (Figures 2B and C, Figure S7). Compared with the wet side, 126 genes were significantly upregulated in the dry side, while 72 genes were significantly downregulated (Figure 2C, Figure S7). Among these, several genes associated with phytohormone abscisic acid (ABA) (Figures 2D and E, Dataset S1 and S2, Figure 3A) were detected. In entire root tips, hydrostimulation upregulated expression of the bZIP transcription factor ABA INSENSITIVE 5 (*SlABI5*), but downregulated the ABA receptor *SlPYL4* (Figure 2D, Dataset S1, Figure 3C and D). While differential expression of these ABA signaling components was not detected in comparing the dry and wet sides of hydrostimulated roots, the dry side generally upregulated the ABA biosynthesis gene *SlABA4* that encodes an enzyme that converts *all-trans*-Violaxanthin into *all-trans* Neoxanthin (Figure 2D and E, Dataset S1 and S2, Figure 3A). qRT-PCR was used to detect ABA-related gene expression in the root tip of control or hydrostimulated plants, or the dry (facing sorbitol) and wet (facing normal 1/2 MS) sides of root tips under hydrostimulation (Figures 3B-D). The expression level of *ABA4* in the dry side was significantly higher than on the wet side (Figure 3B). In addition, hydrostimulation induced the expression levels of *ABI5* (downstream transcription factor of ABA signaling pathway), while decreased expression levels of *PYL4* (a member of ABA receptor family), with no differential expression between wet and dry sides (Figures 3C and D). The qPCR results (Figures 3, Figure S8) are consistent with the RNA seq results (Figure 2, Dataset S1 and S2). Taken together, asymmetric expression of ABA-related genes may be an important mechanism regulating root hydrotropism in tomato.

Arabidopsis thaliana has 12 genes that contain the DUF617 domain that characterises MIZ1-like genes, but only *AtMIZ1* (*At2g41660*) has currently been demonstrated to be required for hydrotropism. A database

(https://solgenomics.net/tools/blast/) search shows that there are 14 MIZ1-like genes in the tomato *genome* (Figure S8A). Among 14 MIZ1-like genes, *Solyc10g080060* gene had the highest ID score of homology with the *Arabidopsis thaliana MIZ1* (Figure S8A). Furthermore, the MIZ1-like gene *Solyc10g080060* (homologous gene of a previously known *Arabidopsis thaliana* hydrotropic gene *AtMIZ1*) was induced by hydrostimulation in entire root tips (Figure 2D, Dataset S1, Figure S8), with greater expression on the dry side than the wet side (Figure 2E, Dataset S2, Figure S8). Quantitative Real time-PCR (qRT-PCR) confirmed that hydrostimulation significantly induced the expression of MIZ1-like gene *Solyc10g080060* in entire root tips, and the expression levels of *Solyc10g080060* in the dry side were also significantly higher than that on the wet side (Figures S8B and C).

3.3 ABA-mediated H^+ efflux plays an important role in tomato root hydrotropism

Adding ABA to the growth medium slightly (but not significantly) increased the degree of hydrotropic curvature (by about 6.5 degrees), while adding FLU to the growth medium significantly decreased the degree of hydrotropic curvature (Figure 4A). In addition, FLU co-treatment with ABA markedly increased the degree of hydrotropic curvature compared to the FLU treatment alone (Figure 4A), suggesting that exogenous ABA can partially reverse to effect of FLU. While the hydrotropic curvature of wild-type tomato was nearly 45 degrees after 10 hours, in the ABA-deficient mutant *not* it was significantly less (about 30 degrees), with these differences detected 6 hours after transplanting the seedlings (Figure 4B). These results further confirmed that ABA positively regulates root hydrotropism in tomato.

Previous studies indicate that ABA levels are closely related to H^+ efflux (Hayashi et al., 2014; Miao et al., 2020; Planes et al., 2015). Using the pH-sensitive dye bromocresol purple (acid-base indicator) (Figures 4C and D) and HPTS staining (a fluorescent pH-indicator) (Figures 4E and F), we determined root tip H^+ efflux in wild-type and ABA-deficient mutant *not* tomato roots under control or hydrostimulated conditions. In the root tips (apical 5 mm), WT and *not* roots had

similar H^+ secretion under control conditions (Figure 4C and D). Although hydrostimulation increased root tip H^+ secretion in both genotypes, an attenuated response occurred in the *not* mutant (Figure 4D). Next, we introduced 8-hydroxypyrene-1,3,6-trisulfonic acid trisodium salt (HPTS) as a suitable fluorescent pH-indicator for assessing apoplastic pH in elongation zone cortex cells in tomato roots (Barbez et al., 2017; Han and Burgess, 2010). Although apoplastic H^+ did not differ between the left and right sides of control WT roots, hydrostimulation significantly increased apoplastic H^+ in the dry side compared to the wet side (Figures 4E and F). Apoplastic H^+ of the ABA-deficient mutant *not* was much less than the WT plants, and independent of whether roots were grown under control or hydrostimulated conditions, with no difference between wet and dry sides (Figures 4E and F). Thus ABA positively regulates asymmetric H^+ efflux in the root tip, which is involved in regulating the hydrotropic response.

4 DISCUSSION

The hydrotropism of terrestrial plant roots has always attracted attention of researchers, and the hydrotropism of roots of plants such as *Arabidopsis*, cucumber, and maize has been extensively studied (Dietrich et al., 2017; Fujii et al., 2018; Chang et al., 2019; Wang et al., 2020). Although an important horticultural crop, *Solanum lycopersicum* root hydrotropism has not yet been examined. This study used a similar system for examining hydrotropism of various tomato cultivars as described by Takahashi et al. (2002). We found that ABA-mediated asymmetric H^+ efflux regulates tomato root hydrotropic bending.

While it has long been known that ABA is involved in regulating the hydrotropic response, since the ABA-deficient *Arabidopsis* mutant *aba1* showed reduced hydrotropism (Takahashi et al. 2002), more recent studies have focused on the role of ABA signaling (specifically the SnRK2.2 kinase) in mediating differential cortical elongation to achieve hydrotropic bending (Dietrich et al. 2017). In tomato, hydrostimulation upregulated the ABA signaling *SlABI5* gene and downregulated the ABA receptor family *PYL4* gene, consistent with previous studies that osmotic stress

induces ABA biosynthesis genes and *ABI5* gene expression but inhibits ABA receptor family gene expression (Thompson et al., 2000; Wan and Li, 2006; Sun et al., 2011; Chen et al., 2017). In tomato roots responding to a water potential (Ψ) gradient, the ABA biosynthesis *SlABA4* gene was differentially expressed between dry and wet sides (Figure 3), implying local sensing of substrate water potential. In addition, hydrostimulation induced H^+ efflux (Figures 4C and D), causing asymmetric H^+ efflux that enhances cell elongation on the dry side of the root, allowing the root to bend towards the wet side to take up more water. Taken together, these observations suggest multiple changes in gene expression within the root tip to adapt to substrate Ψ gradients, although it is difficult to distinguish between local (ABA biosynthesis independently responding to local changes in Ψ) *versus* co-ordinated (mobile ABA signals within the root) responses.

Whereas *Arabidopsis* showed a strong hydrotropic response when grown on a water potential gradient formed by 400 mM sorbitol (Takahashi et al., 2002), a higher sorbitol concentration (1000 mM) was the most suitable to study tomato plants as substantial root bending occurred with minimal root growth inhibition (Figures S1 and S2). Despite these species differences in sensitivity to hydrostimulation, there was minimal variation between tomato cultivars, with only the dwarf cultivar Micro-Tom showing less curvature (Figure S5). Under hydrostimulation, the dry side of the roots contain more meristematic cortex cells and longer elongation zone cortex cells than the wet side (Figures 1B-D). These cellular responses are consistent with previous studies on *Arabidopsis* (Dietrich et al., 2017; Chang et al., 2019) and maize (*Zea mays*) (Wang et al., 2020). Therefore, compared with the wet side, the dry side of the roots has more cortex cell number and faster cell growth, which leads to the root bending towards water.

Previous studies indicated that *Mizu-kussei 1* (*MIZ1*) is crucial for root hydrotropism (Kobayashi al., 2007). By directly interacting with the endoplasmic reticulum (ER) Ca^{2+}-ATPase isoform ECA1, MIZ1 causes an asymmetrical distribution of Ca^{2+} in the elongation zone of *Arabidopsis* roots prior to hydrotropic bending (Shkolnik et al., 2018). Although *MIZ1* expression is crucial for responding

to moisture gradients, previously there was no direct evidence for its asymmetric expression in roots under hydrostimulation (Moriwaki et al., 2010; Fujii et al., 2018). Hydrostimulation significantly upregulates *MIZ1* expression in whole tomato root tips (Figures 2B and D; Dataset S1; Figure S8), and results in its asymmetric expression on either side of the root tip, determined by collecting samples from root tips that were split longitudinally into two halves (Figures 2C and E; Dataset S2; Figure S8). Thus asymmetric expression of *MIZ1* is involved in tomato root hydrotropic bending, providing further evidence for the important role of *MIZ1* in root hydrotropism.

MIZ1 was not the only gene showing differential expression between either side of hydrostimulated root tips, with the core components of ABA signaling also affected (Figure 2D). While early work highlighted the role of the *Arabidopsis aba1* gene (which encodes zeaxanthin epoxidase) in mediating root hydrotropism (Takahashi et al., 2002), the ABA biosynthesis gene *SlABA4* (the next step in the ABA biosynthesis pathway) was asymmetrically expressed on both sides of tomato root tips under hydrostimulation (Figure 2E; Figure 3B), with *ABA4* levels higher on the dry side of the root than the wet side. The functional significance of differential gene expression (and presumably ABA levels) was further examined by measuring the hydrotropic responses of the ABA-deficient tomato mutant *notabilis (not)*, which has a lesion in the *SlNCED1* (9-cis-epoxycarotenoid dioxygenase) gene (Burbidge et al. 1999) resulting in 27% lower root ABA concentrations when grown *in vitro* (Belimov et al. 2014). Consistent with the presumed role of ABA in mediating hydroptropism, *not* showed less hydrotropic response (Figure 4B), as did WT roots treated with an ABA biosynthesis inhibitor (Figure 4A). Thus both mutational and pharmacological approaches showed that the ABA is involved in tomato root hydrotropism.

In roots, whilst high exogenous ABA levels inhibit growth (Fujii et al., 2007), moderate ABA levels promote elongation by regulating PM H^+-ATPase-mediated H^+ efflux at low water potential (Janicka-Russak and Kłobus, 2007; Xu et al., 2013). Moreover, the PM H^+-ATPase-mediated H^+ efflux promotes root hydrotropism in *Arabidopsis thaliana* (Miao et al., 2018; Miao et al., 2020). Hydrostimulation increased H^+ efflux but to a lesser extent in the ABA deficient *not* mutant (Figures 4C

and D). Cell wall acidification mediated by H^+ efflux enhances cellular elongation (Moloney et al., 1981; Hager, 2003; Falhof et al., 2016). Thus, the asymmetric distribution of apoplastic H^+ was positively correlated with asymmetric cell growth (Figures 1B-D; Figures 4E and F). Taken together, these results suggest that ABA positively regulates asymmetric H^+ efflux in the root tip, which enhances cell elongation to ensure root hydrotropic bending.

In conclusion, our results suggest that ABA-mediated asymmetric H^+ efflux is required for root hydrotropism. The expression of ABA-related genes on the dry side of the root are increased under hydrostimulation, and the enhanced H^+ efflux promotes root hydrotropic bending (Figure 5). Uncovering the detailed physiological and molecular mechanisms of differential ABA response-mediated root hydrotropism may help develop novel strategies to generate more productive crop plants when soil moisture is heterogenous.

AUTHOR CONTRIBUTIONS

Li Y., Chen Y., Yuan W. and Xu W. conceived and designed the experiments; Chen Y., Jiang S., Dai H. and Zhang Q. performed the experiments; Jiang S. and Yuan W. analysed the data. Li Y., Zhang J., Xu W. and Dodd I.C. wrote the paper.

ACKNOWLEDGEMENTS

We are grateful for grant support from the National Key Research and Development Program of China (2022YFD1900705), Natural Science Foundation of Jiangsu Province (BK20220566), the China Postdoctoral Science Foundation (2023M733003) and the National Natural Science Foundation of China (31872169, 31761130073 and 31422047). We are also grateful for a Project Funded by the Priority Academic Program Development of Jiangsu Higher Education Institutions (PAPD) and a Newton Advanced Fellowship (NSFC-RS: NA160430). We thank Dr. Lin Chen (Yangzhou University) for providing the MM seeds.

CONFLICT OF INTEREST

The authors declare no conflict of interest.

DATA AVAILABILITY STATEMENT

The data that support the findings of this study are openly available. The RNA

505 sequencing data generated in this study have been deposited in the National Centre for
506 Biotechnology Information (NCBI) (http://www.ncbi.nlm.nih.gov/) with the
507 Bioproject of PRJNA910593.

508 **REFERENCES**

509 Antoni, R., Gonzalez-Guzman, M., Rodriguez, L., Peirats-Llobet, M., Pizzio, G.A.,
510 Fernandez, M.A. et al. (2013) PYRABACTIN RESISTANCE1-LIKE8 Plays an
511 Important Role for the Regulation of Abscisic Acid Signaling in Root. *Plant*
512 *Physiology*, 161, 931-941.

513 Barbez, E., Dünser, K., Gaidora, A., Lendl, T. & Busch, W. (2017) Auxin steers root
514 cell expansion via apoplastic pH regulation in *Arabidopsis thaliana*. *Proceedings*
515 *of the National Academy of Sciences*, USA, 114, E4884-E4893.

516 Belimov, A.A., Dodd, I.C., Safronova, V.I., Dumova, V.A., Shaposhnikov, A.I.,
517 Ladatko, A.G. et al. (2014) Abscisic acid metabolizing rhizobacteria decrease
518 ABA concentrations in *planta* and alter plant growth. *Plant Physiology and*
519 *Biochemistry*, 74, 84-91.

520 Bissoli, G., Niñoles, R., Fresquet, S., Palombieri, S., Bueso, E., Rubio, L. et al.
521 (2012) Peptidyl-prolyl *cis-trans* isomerase ROF2 modulates intracellular pH
522 homeostasis in *Arabidopsis*. *The Plant Journal*, 70, 704-716.

523 Burbidge, A., Grieve, T.M., Jackson, A., Thompson, A., McCarty, D.R. & Taylor, I.B.
524 (1999) Characterization of the ABA-deficient tomato mutant *notabilis* and its
525 relationship with maize *Vp14*. *The Plant Journal*, 17, 427-31.

526 Chang, J., Li, X., Fu, W., Wang, J., Yong, Y., Shi, H. et al. (2019) Asymmetric
527 distribution of cytokinins determines root hydrotropism in *Arabidopsis thaliana*.
528 *Cell Research*, 29, 984-993.

529 Chen, Y., Feng, L., Wei, N., Liu, Z.H., Hu, S., Li, X.B. (2017) Overexpression of
530 cotton PYL genes in Arabidopsis enhances the transgenic plant tolerance to
531 drought stress. Plant Physiology and Biochemistry, 115, 229-238.

532 Dietrich, D., Pang, L., Kobayashi, A., Fozard, J.A., Boudolf, V., Bhosale, R. et al.
533 (2017) Root hydrotropism is controlled via a cortex-specific growth mechanism.

534 *Nature Plants*, 3, 17057.
535 Eapen, D., Martínez-Guadarrama, J., Hernández-Bruno, O., Flores, L., Nieto-Sotelo,
536 J., Cassab, G.I. (2017) Synergy between root hydrotropic response and root
537 biomass in maize (*Zea mays* L.) enhances drought avoidance. *Plant Science*, 265,
538 87-99.
539 Falhof, J., Pedersen, J.T., Fuglsang, A.T. & Palmgren, M. (2016) Plasma Membrane
540 H^+-ATPase Regulation in the Center of Plant Physiology. *Molecular Plant*, 9,
541 323-337.
542 Fujii, H., Verslues, P.E., & Zhu, J.K. (2007) Identification of Two Protein Kinases
543 Required for Abscisic Acid Regulation of Seed Germination, Root Growth, and
544 Gene Expression in *Arabidopsis*. *The Plant Cell*, 19, 485-494.
545 Fujii, N., Miyabayashi, S., Sugita, T., Kobayashi, A., Yamazaki, C., Miyazawa, Y. et
546 al. (2018) Root-tip-mediated inhibition of hydrotropism is accompanied with the
547 suppression of asymmetric expression of auxin-inducible genes in response to
548 moisture gradients in cucumber roots. *PLoS One*, 13, e0189827.
549 Furihata, T., Maruyama, K., Fujita, Y., Umezawa, T., Yoshida, R., Shinozaki, K. et al.
550 (2006) Abscisic acid-dependent multisite phosphorylation regulates the activity
551 of a transcription activator AREB1. *Proceedings of the National Academy of*
552 *Sciences*, USA, 103, 1988-1993.
553 Hager, A. (2003) Role of the plasma membrane H^+-ATPase in auxin-induced
554 elongation growth: historical and new aspects. *Journal of Plant Research*, 116,
555 483-505.
556 Han, J. & Burgess, K. (2010) Fluorescent Indicators for Intracellular pH. *Chemical*
557 *Reviews*, 110, 2709-2728.
558 Hayashi, Y., Takahashi, K., Inoue, S.I. & Kinoshita, T. (2014) Abscisic Acid
559 Suppresses Hypocotyl Elongation by Dephosphorylating Plasma Membrane
560 H^+-ATPase in *Arabidopsis thaliana*. *Plant and Cell Physiology*, 55(4), 845-853.
561 Iwata, S., Miyazawa, Y., Fujii, N., Takahashi, H. (2013) MIZ1-regulated
562 hydrotropism functions in the growth and survival of *Arabidopsis thaliana* under
563 natural conditions. *Annals of Botany*, 112, 103-114.

564 Janicka-Russak, M. & Kłobus, G. (2007) Modification of plasma membrane and
565 vacuolar H^+-ATPases in response to NaCl and ABA. *Journal of Plant*
566 *Physiology*, 164, 295-302.
567 Kobayashi, A., Takahashi, A., Kakimoto, Y., Miyazawa, Y., Fujii, N., Higashitani, A.
568 et al. (2007) A gene essential for hydrotropism in roots. *Proceedings of the*
569 *National Academy of Sciences*, USA, 104, 4724-4729.
570 Li, Y., Yuan, W., Li, L., Dai, H., Dang, X., Miao, R. et al. (2020 a) Comparative
571 analysis reveals gravity is involved in the MIZ1-regulated root hydrotropism.
572 *Journal of Experimental Botany*, 71, 7316-7330.
573 Li, Y., Yuan, W., Li, L., Miao, R., Dai, H., Zhang, J. et al. (2020 b) Light-Dark
574 modulates root hydrotropism associated with gravitropism by involving
575 amyloplast response in *Arabidopsis*. *Cell Reports*, 32(13), 108-198.
576 Li, Y., Zeng, H., Xu, F., Yan, F. & Xu, W. (2022) H^+-ATPases in plant growth and
577 stress responses. *Annual Review of Plant Biology*, 73, 495-521.
578 Ma, Y., Szostkiewicz, I., Korte, A., Moes, D., Yang, Y., Christmann, A. et al. (2009)
579 Regulators of PP2C phosphatase activity function as abscisic acid sensors.
580 *Science*, 324, 1064-1068.
581 Miao, R., Wang, M., Yuan, W., Ren, Y., Li, Y., Zhang, N. et al. (2018) Comparative
582 Analysis of *Arabidopsis* Ecotypes Reveals a Role for Brassinosteroids in Root
583 Hydrotropism. *Plant Physiology*, 176, 2720-2736.
584 Miao, R., Yuan, W., Wang, Y., Garcia-Maquilon, I., Dang, X., Li, Y. et al. (2020)
585 Low ABA concentration promotes root growth and hydrotropism through relief
586 of ABA INSENSITIVE 1-mediated inhibition of plasma membrane H^+-ATPase
587 2. *Science advances*, 7, eabd4113.
588 Moloney, M.M., Elliott, M.C. & Cleland, R.E. (1981) Acid growth effects in maize
589 roots: Evidence for a link between auxin-economy and proton extrusion in the
590 control of root growth. *Planta*, 152, 285-291.
591 Moriwaki, T., Miyazawa, Y., Fujii, N. & Takahashi, H. (2012) Light and abscisic acid
592 signalling are integrated by MIZ1 gene expression and regulate hydrotropic
593 response in roots of *Arabidopsis thaliana*. *Plant Cell & Environment*, 35,

1359-1368.

Moriwaki, T., Miyazawa, Y. & Takahashi, H. (2010) Transcriptome analysis of gene expression during the hydrotropic response in *Arabidopsis* seedlings. *Environmental and Experimental Botany*, 69, 148-157.

Nishimura, N., Hitomi, K., Arvai, A.S., Rambo, R.P., Hitomi, C., Cutler, S.R. et al. (2009) Structural mechanism of abscisic acid binding and signaling by dimeric PYR1. *Science*, 326, 1373-1379.

Park, S.Y., Fung, P., Nishimura, N., Jensen, D.R., Fujii, H., Zhao, Y. et al. (2009) Abscisic acid inhibits type 2C protein phosphatases via the PYR/PYL family of START proteins. *Science*, 324, 1068-1071.

Planes, M.D., Niñoles, R., Rubio, L., Bissoli, G., Bueso, E., García-Sánchez, M.J. et al. (2015) A mechanism of growth inhibition by abscisic acid in germinating seeds of *Arabidopsis thaliana* based on inhibition of plasma membrane H^+-ATPase and decreased cytosolic pH, K^+, and anions. *Journal of Experimental Botany*, 66, 813-825.

Rowe, J.H., Topping, J.F., Liu, J. & Lindsey, K. (2016) Abscisic acid regulates root growth under osmotic stress conditions via an interacting hormonal network with cytokinin, ethylene and auxin. *New Phytologist*, 211, 225-239.

Sharp, R.E., Wu, Y., Voetberg, G.S., Saab, I.N. & Lenoble, M.E. (1994) Confirmation that abscisic acid accumulation is required for maize primary root elongation at low water potentials. *Journal of Experimental Botany*, 45, 1743-1751.

Shkolnik, D., Nuriel, R., Bonza, M.C., Costa, A. & Fromm, H. (2018) MIZ1 regulates ECA1 to generate a slow, long-distance phloem-transmitted Ca^{2+} signal essential for root water tracking in *Arabidopsis*. *Proceedings of the National Academy of Sciences*, USA, 115, 8031-8036.

Sun, L., Wang, Y.P., Chen, P., Ren, J., Ji, K., Li, Q. et al. (2011) Transcriptional regulation of SlPYL, SlPP2C, and SlSnRK2 gene families encoding ABA signal core components during tomato fruit development and drought stress. Journal of Experimental Botany, 62, 5659-69.

624 Takahashi, N., Goto, N., Okada, K. & Takahashi, H. (2002) Hydrotropism in abscisic
625 acid, wavy, and gravitropic mutants of *Arabidopsis thaliana*. *Planta*, 216,
626 203-211.
627 Thompson, A.J., Jackson, A.C., Parker, R.A., Morpeth, D.R., Burbidge, A., Taylor,
628 I.B. (2000) Abscisic acid biosynthesis in tomato: regulation of zeaxanthin
629 epoxidase and 9-cis-epoxycarotenoid dioxygenase mRNAs by light/dark cycles,
630 water stress and abscisic acid. Plant Molecular Biology, 42, 833-45.3
631 Umezawa, T., Sugiyama, N., Takahashi, F., Anderson, J.C., Ishihama, Y., Peck, S.C.,
632 Shinozaki, K. (2013) Genetics and phosphoproteomics reveal a protein
633 phosphorylation network in the abscisic acid signaling pathway in *Arabidopsis*
634 *thaliana*. Science Signal, 6,rs8.
635 Uno, Y., Furihata, T., Abe, H., Yoshida, R., Shinozaki, K. & Yamaguchi-Shinozaki,
636 K. (2000) *Arabidopsis* basic leucine zipper transcription factors involved in an
637 abscisic acid-dependent signal transduction pathway under drought and
638 high-salinity conditions. *Proceedings of the National Academy of Sciences*, USA,
639 97, 11632-11637.
640 Wan, X.R., Li, L. (2006) Regulation of ABA level and water-stress tolerance of
641 Arabidopsis by ectopic expression of a peanut 9-cis-epoxycarotenoid
642 dioxygenase gene. Biochemical and Biophysical Research Communications, 347,
643 1030-1038.
644 Wang, P., Xue, L., Batelli, G., Lee, S., Hou, Y.J., Van, Oosten M.J., Zhang, H., Tao,
645 W.A., Zhu, J-K. (2013) Quantitative phosphoproteomics identifies SnRK2
646 protein kinase substrates and reveals the effectors of abscisic acid action.
647 *Proceedings of the National Academy of Sciences*, USA, 110, 11205-11210.
648 Wang, Y., Afeworki, Y., Geng, S., Kanchupati, P., Gu, M., Martins, C. et al. (2020)
649 Hydrotropism in the primary roots of maize. *New Phytologist*, 226, 1796-1808.
650 Xu, W., Jia, L., Shi, W., Liang, J., Zhou, F., Li, Q. et al. (2013) Abscisic acid
651 accumulation modulates auxin transport in the root tip to enhance proton
652 secretion for maintaining root growth under moderate water stress. *New*
653 *Phytologist*, 197, 139-150.

SUPPORTING INFORMATION

Supplementary Table 1. Specific gene primers for qRT-PCR.

Supplementary Dataset 1. Fold changes and P-values of differentially expressed genes in the root tips under hydrostimulation compared with under control conditions determined by RNA-seq.

Supplementary Dataset 2. Fold changes and P-values of differentially expressed genes in the dry side compared with the wet side of hydrostimulated root tips determined by RNA-seq.

Supplement Figure 1. Diagram illustrating the agar-sorbitol system used for testing root hydrotropism.

Supplement Figure 2. Hydrotropism of tomato root under the different water potential gradients.

Supplement Figure 3. Changes in agar water potential at various distances from the plain agar-sorbitol (1000 mM) agar junction in the agar-sorbitol system.

Supplement Figure 4. Changes in root hydrotropism of tomato wild-type (LU) in the agar-1000 mM sorbitol system.

Supplement Figure 5. Hydrotropism of different tomato ecotypes (Micro-Tom = MT, Moneymaker = MM, Lukullus = LU, and Ailsa Craig = AC).

Supplement Figure 6. Transcriptomic data analysis from RNA sequencing with Pearson correlation heatmap between each sample (A) and hierarchical clustering of the differentially expressed genes among treatments (B).

Supplement Figure 7. RNA-sequencing showing differentially expressed genes between treatments.

Supplement Figure 8. The MIZ1-like genes in tomato and the MIZ1-like gene *Solyc10g080060* expression in the apical 5 mm of tomato root tips under hydrostimulation.

Figure legends

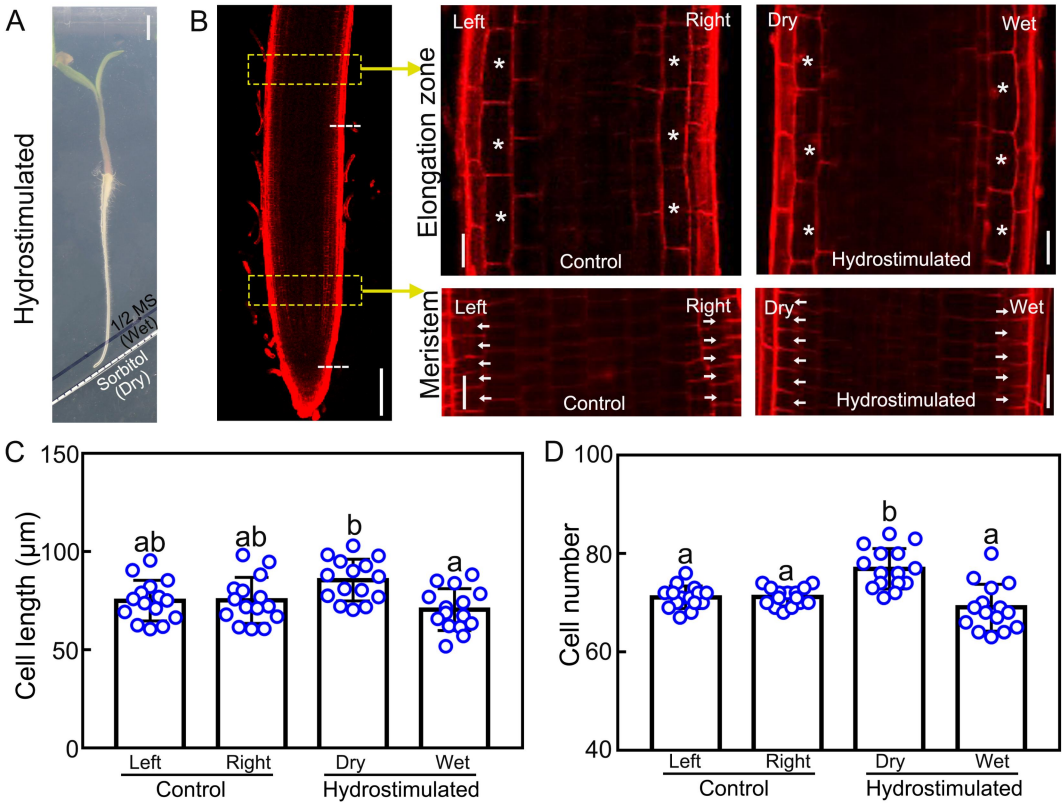

FIGURE 1 Differential cortex cell elongation and cortex cell number of both sides (dry side and wet side) of tomato wild-type (Lukullus) root tips under hydrostimulation.

(A) Representative images of tomato roots hydrostimulated for 12 h. The white dotted line is the border between 1/2 MS conditions (wet) and sorbitol (dry), and the black solid line indicates the original position of the root tip when transferring from normal 1/2 MS conditions. Scale bar: 4 mm. (**B**) The cortex cell length on both sides in elongation zone or cortex cell number in meristematic zone of tomato root tip under control conditions or hydrostimulated for 3 h. Root meristem depicted as the distance between the QC/root cap border and the onset of rapid cell elongation(white dashed lines), and QC/root cap border was used as a starting point for the meristem cell count and the onset of rapid cell elongation was used as an ending point for the meristem cell count. Root elongation zone depicted as the distance between the onset of rapid cell elongation and the first root hair bulge in the epidermis, and onset of rapid cell elongation was used as a starting point for the elongation zone cell length and the first

root hair bulge in the epidermis was used as an ending point for the elongation zone cortex cell length. The cells enclosed in the boxes were used for cell length in elongation zone or cell number in meristematic zone measurement as an example. Asterisks denote cortex cells on both sides of the elongation zone, and arrows denote cortex cells on both sides of meristematic zone. Dry, the side facing sorbitol; Wet, the side facing normal 1/2 MS. Roots were stained with PI. Scale bar in the left figure: 200 μm. Scale bar in the left figure: 40 μm. (**C** and **D**) Quantification of cortex cell length (**C**) in elongation zone or cortex cell number in meristematic zone (**D**) in the roots of plants described in (**B**) (n = 15 roots). Each symbol is an individual root (C and D), with data presented as means ± SE of three independent experiments; different letters denote significant differences ($P < 0.05$, Tukey's test).

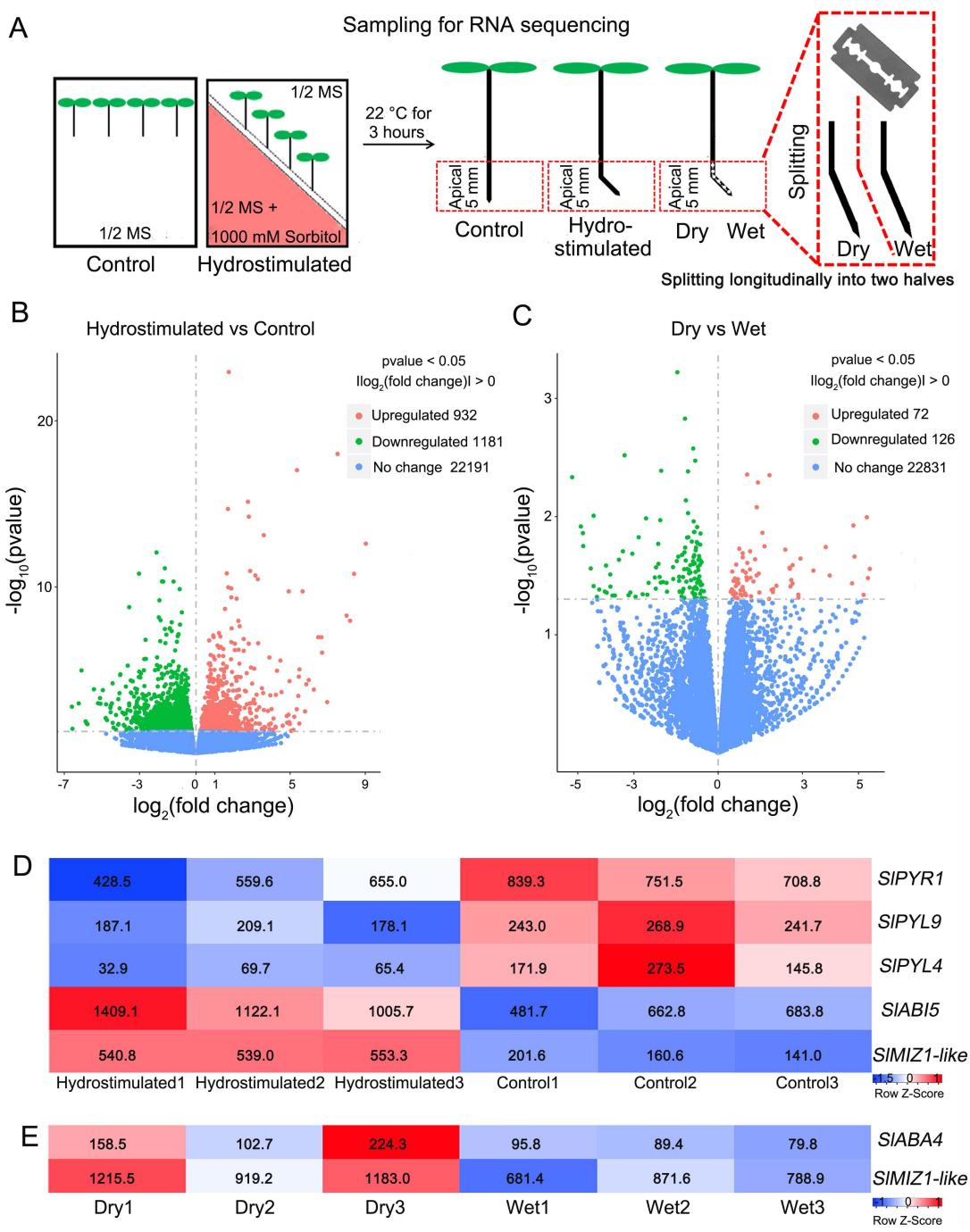

FIGURE 2 Response of ABA pathway genes at the apical 5 mm of both dry and wet sides of tomato root tips under hydrostimulation.

(**A**) Flow chart of RNA sequencing for harvesting samples in the apical 5 mm of tomato root tips. Control roots are grown under normal 1/2 MS conditions, while in hydrostimulated roots the dry side is facing sorbitol and the wet side is facing normal 1/2 MS. (**B** and **C**) Relationship between average expression of control vs hydrostimulated whole root tips (**B**) and dry vs wet sides (**C**) and fold change for each

gene. Each dot in the graphs represents a single gene, and red represents upregulated differentially expressed genes (DEGs), green represents downregulated DEGs, and blue represents no change. (**D** and **E**) Heatmap visualizing the expression patterns of DEGs in the ABA-related pathway in the apical 5 mm of tomato root tips under hydrostimulation. The apical 5 mm of tomato root tips were obtained after 3 h of control or hydrostimulation. ABA-related genes are differentially expressed. Each row represents one gene, columns represent the different treatments, and low expression levels are in blue and high expression levels are in red. *PYR*, Pyrabactin resistance1; *PYL*, PYR1-like; *ABI5*, ABA insensitive 5; *ABA4*, ABA deficient 4; *MIZ1-like*, MIZU-KUSSEI-like (*Solyc10g080060*).

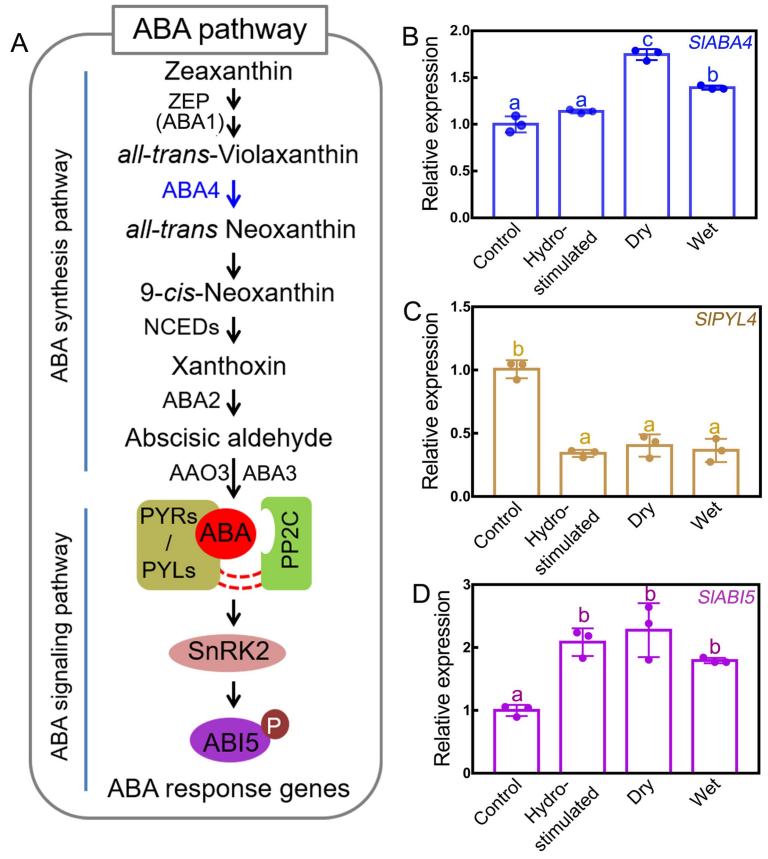

766

767 **FIGURE 3 ABA-related genes are differentially expressed in the apical 5 mm**
768 **area of dry and wet sides of tomato root tips under hydrostimulation.**

769 (**A**) Schematic overview of ABA synthesis and signalling pathway, with expression of
770 the *SlABA4* (**B**), *SlPYL4* (**C**) and *SlABI5* (**D**) genes in the apical 5 mm of tomato root
771 tips after 3 h control or hydrostimulation. Gene expression (**B-D**) under control
772 conditions was taken as 100%, relative gene expression under hydrostimulation were
773 calculated relative to control levels. *α-Tubulin* was used as the internal control.
774 Control roots are the root tips under normal 1/2 MS conditions; hydrostimulated roots
775 are the root tips under hydrostimulation; with the dry side facing sorbitol and the wet
776 side facing normal 1/2 MS under hydrostimulation. Data in **B-D** are presented as
777 means ± SE of three independent biological replicates; different letters denote
778 significant differences (P<0.05, Tukey's test).

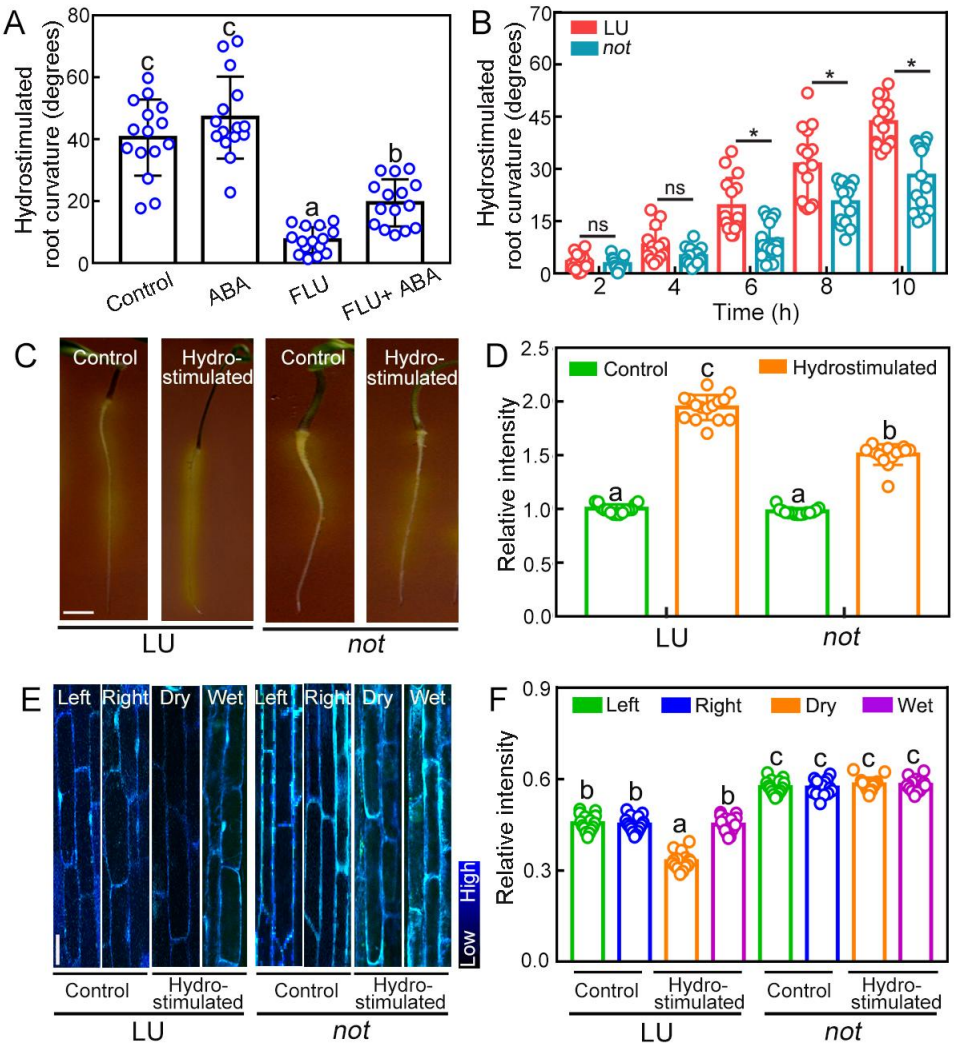

779

780 **FIGURE 4 ABA-mediated asymmetric H^+ efflux positively regulates the**
781 **hydrotropism of tomato root.**

782 (**A**) Hydrotropic bending of tomato wild-type (LU) roots under control, 1 µM ABA
783 and 10 µM FLU (fluridone, ABA biosynthetic inhibitor) treatments after 10 h of
784 hydrostimulation (n = 15 roots). (**B**) Hydrotropic bending of wild-type and the ABA
785 deficient mutant *not* (n = 15 roots). (**C**) Representative images of wild-type and ABA
786 deficient mutant *not* roots stained with pH indicator bromocresol purple after 3 h
787 control or hydrostimulation. A yellow colour around the roots indicates proton (H^+)
788 extrusion. Scale bar: 6 mm. (**D**) Quantification of proton (H^+) extrusion in the apical 5
789 mm of root tips of wild-type LU and ABA deficient mutant *not* (n = 15 roots). (**E**)
790 Representative images for HPTS staining of wild-type and ABA deficient mutant *not*
791 apoplastic epidermal and cortical cells in root elongation zone after 3 h control or

hydrostimulation. Control roots grew on normal 1/2 MS conditions without water potential gradient, while hydrotimulated roots grew on agar-sorbitol system with a water potential gradient with the dry side facing sorbitol and the wet side facing normal 1/2 MS. Scale bar: 25 μm. Color code (black to blue) describes (low to high) 458/405 intensity and pH values. (**F**) Quantification of H^+ efflux in the root of plants described in (**E**) (n = 15 roots). Each symbol is an individual root. The relative intensity correlate with the 458/405 ratio values. The higher the 458/405 ratio, the higher the pH and less apoplastic H^+. Data in **A**, **B**, **D** and **F** are presented as means ± SE of three independent experiments; different letters denote significant differences ($P < 0.05$, Tukey's test).

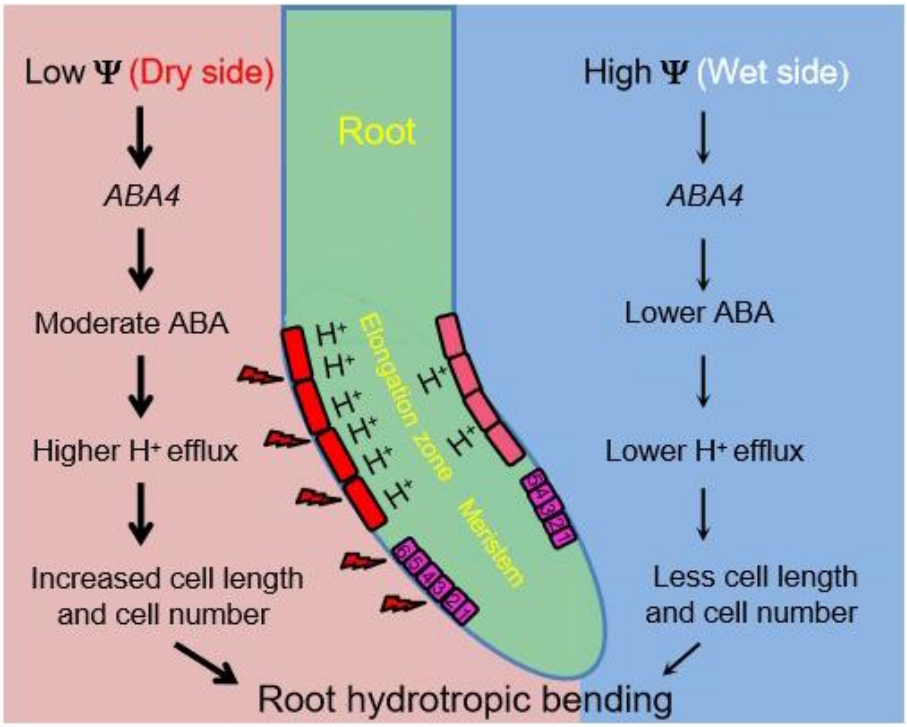

822

823 **FIGURE 5 Proposed model illustrating the involvement of ABA-mediated**
824 **asymmetric H^+ efflux in root hydrotropism.**

825 Compared to the wet side of the root tip at higher water potential, the dry side at lower
826 water potential induces the expression of ABA biosynthesis gene *ABA4*, thus
827 enhancing proton efflux to promote cell elongation on the dry side. In addition, the
828 cortex cell numbers on the dry side are higher than on the wet side. Because H^+ efflux
829 and cell elongation on the dry side of the root tip are higher than on the wet side,
830 asymmetric growth allows the root to bend towards the wet side to take up more
831 water.

832

833

834

835

836

837

838

839